Principles of Echolocation
in Bats and Machines

Note 10

Why LAEAP?

Drawing sonar images, beampatterns and HRTFs on a flat page

Jan Steckel
Cosys-Lab, University of Antwerp, and Flanders Make, Belgium jan.steckel@uantwerpen.be

Version 2026-11-18 16:30

1 A Hemisphere on Paper

A 3D sonar such as our eRTIS sends out a call and listens with a planar array of microphones. After beamforming, it knows how much echo energy came from every direction in front of it, so its image lives on a hemisphere. The same is true for the beampattern of an array and for the head-related transfer function (HRTF) of a bat, which tells how loud a sound from each direction is heard in one ear. All three have to end up on a flat page or screen.

Gauss proved in 1827 that a sphere cannot be flattened without distortion. A map can keep some properties of the sphere, but never all of them at once, so every map is a choice. The most common choice in sonar and acoustics is the simplest one: put azimuth on the horizontal axis, elevation on the vertical axis, and fill the rectangle. In all our notes, we use a different map, the Lambert azimuthal equal-area projection (LAEAP), which shows the frontal hemisphere as a disc. In this note we explain why. We first look at where a beampattern naturally lives, then at how the rectangular map distorts it, derive the LAEAP step by step, and see what its equal-area property buys when we beamform and when we read an image. We also say honestly what it does not keep.

Throughout, we use the conventions of the series. The sensor looks along x, y is its left and z is up. A direction with azimuth ϕ (positive to the left) and elevation θ (positive up) is the unit vector

$$\boldsymbol{d} = (\cos\theta\cos\phi,\ \cos\theta\sin\phi,\ \sin\theta). \tag{1}$$

The poles of this system, $\theta = \pm 90°$, are straight up and straight down.

2 Where a Beampattern Lives

Take a planar array in the y-z plane, with microphone n at $\boldsymbol{p}_n = (0, y_n, z_n)$. A plane wave from direction $\boldsymbol{d}$ reaches microphone n earlier than the array centre by $\boldsymbol{p}_n \cdot \boldsymbol{d}/c$, which gives a phase of $2\pi\, \boldsymbol{p}_n \cdot \boldsymbol{d}/\lambda$ at wavelength λ. Because the microphones have no x coordinate, only two components of $\boldsymbol{d}$ enter this phase,

$$u = d_y = \cos\theta\sin\phi, \qquad v = d_z = \sin\theta. \tag{2}$$

These are the direction cosines of $\boldsymbol{d}$ with respect to the y and z axes. Delay-and-sum beamforming steered to $\boldsymbol{d}_0$, with direction cosines (u_0, v_0), removes the phases of that direction and

averages, which gives the beampattern

$$B(u,v) = \left| \frac{1}{N} \sum_{n=1}^{N} e^{j2\pi[y_n(u-u_0)+z_n(v-v_0)]/\lambda} \right|. \tag{3}$$

The pattern depends only on the differences $u-u_0$ and $v-v_0$. Steering the beam therefore slides one fixed shape across the (u,v) plane without changing it: the beampattern is shift-invariant in direction cosines. Only the part of the plane with $u^2+v^2 \le 1$ corresponds to real directions, since $\boldsymbol{d}$ is a unit vector. For an $M \times M$ uniform rectangular array with spacing d, the sum in equation (3) splits into two geometric series, one in u and one in v, and

$$B(u,v) = \left| \frac{\sin\left(M\pi d(u-u_0)/\lambda\right)}{M\sin\left(\pi d(u-u_0)/\lambda\right)} \right| \left| \frac{\sin\left(M\pi d(v-v_0)/\lambda\right)}{M\sin\left(\pi d(v-v_0)/\lambda\right)} \right|. \tag{4}$$

Our example throughout this note is such an array with $M = 8$ and $d = \lambda/2$, steered straight ahead (broadside) and to $\phi_0 = 55°$, $\theta_0 = 45°$. That second direction has $(u_0, v_0) = (0.58, 0.71)$ and lies 66° from boresight.

Figure 1 shows both beams in three maps. In direction cosines (b), the two beams are the same pattern, shifted. In the rectangular azimuth/elevation map (a), the steered beam looks like a different object: the mainlobe is a long, bent banana, and the sidelobes near the top are smeared over the whole width of the map. The reason is the top edge of that map. Every point on it, from $\phi = -90°$ to $90°$, is the same direction, straight up. A single direction has been stretched into a line. The LAEAP disc (c) keeps the mainlobe compact, shows the whole hemisphere without an edge at the poles, and, as we will see, draws every part of the pattern at its true size.

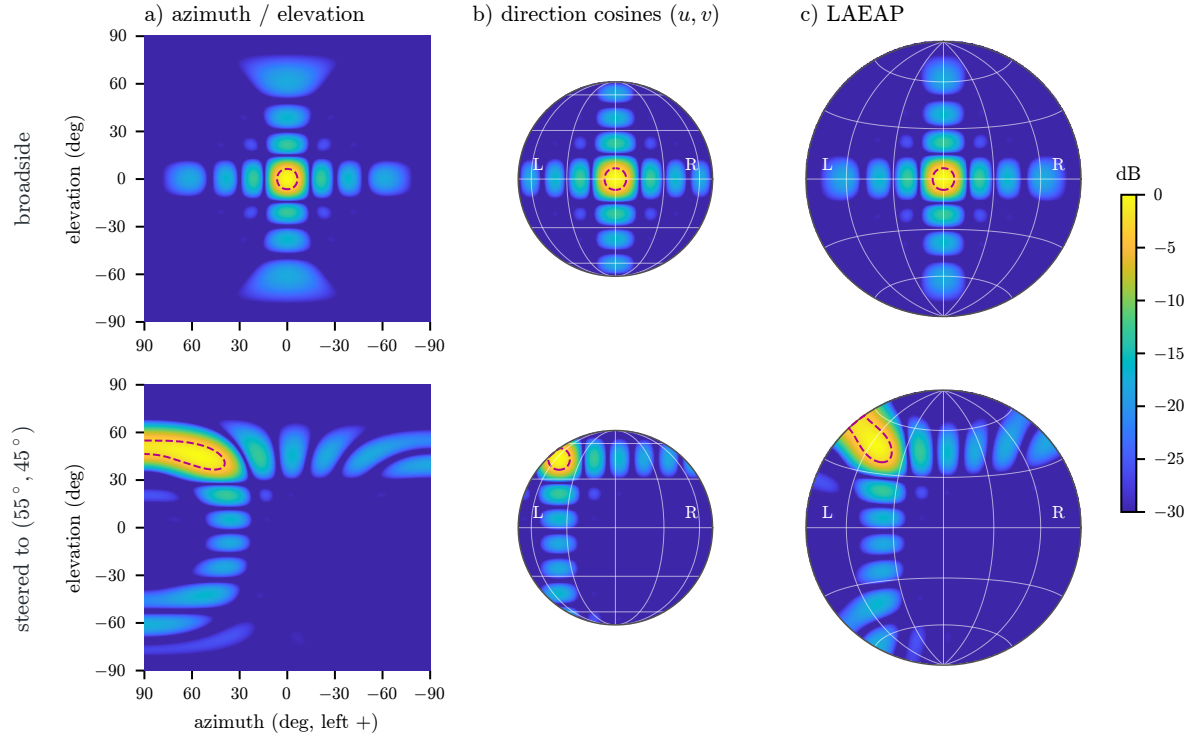


Figure 1: The beampattern of an 8×8 array with half-wavelength spacing, broadside (top) and steered to $(55°, 45°)$ (bottom), in three maps of the frontal hemisphere, all seen from behind the sensor (L and R mark its left and right) and drawn at the same scale. a) Azimuth against elevation. b) Direction cosines (u, v), the unit disc. c) LAEAP, a disc of radius $\sqrt{2}$. The magenta contour is the −3 dB mainlobe, the white grid lines are 30° apart in azimuth and elevation.

If the (u, v) plane is so natural for a planar array, why not use it as our map? Look at the rim of the disc in Fig. 1b. Directions close to 90° from boresight are squeezed into a thin ring, because u and v hardly change when $\boldsymbol{d}$ approaches the y-z plane. A small patch of the sphere around $\boldsymbol{d}$ is projected onto the y-z plane at an angle, and its area shrinks by the cosine of the angle t between $\boldsymbol{d}$ and the x axis:

$$du\,dv = \cos t\; d\Omega, \qquad \cos t = d_x = \sqrt{1 - u^2 - v^2}. \tag{5}$$

At 66° from boresight, a patch of sky appears at only 0.41 of its true size. The direction-cosine map hides the fact that a steered beam really covers more directions than a broadside one.

3 How Much Sky Is in a Pixel?

To compare maps, we need the size of a patch of directions, the solid angle Ω, measured in steradians. It is the area of the patch on the unit sphere. The whole sphere has 4π sr, the frontal hemisphere 2π sr.

Take a small cell of the rectangular map, $d\phi$ wide and $d\theta$ high. A step $d\theta$ in elevation moves $\boldsymbol{d}$ along a meridian, a great circle of radius 1, so it covers an arc of length $d\theta$ on the unit sphere. A step $d\phi$ in azimuth moves $\boldsymbol{d}$ along a circle of constant elevation. That circle has radius $\cos\theta$ (the distance of $\boldsymbol{d}$ from the vertical axis, from equation (1)), so the arc is only $\cos\theta\, d\phi$ long. The cell therefore holds the solid angle

$$d\Omega = \cos\theta\; d\phi\, d\theta, \tag{6}$$

while it takes up the area $d\phi\, d\theta$ on the map. The rectangular map draws a patch of sky $1/\cos\theta$ times too large: 1.15 times at 30° elevation, 2.0 times at 60°, 5.8 times at 80°, and infinitely large at the poles (Fig. 2c).

For cells of finite size, we integrate equation (6). A cell from θ_1 to θ_2 and $\Delta\phi$ wide holds $\Delta\phi\,(\sin\theta_2 - \sin\theta_1)$. A 15° cell at the horizon holds $\Delta\phi \sin 15° = 68$ msr, the cell next to the pole only $\Delta\phi\,(1 - \sin 75°) = 8.9$ msr, 7.6 times less. On the rectangular map, both are drawn the same size (Fig. 2a). Seen differently, the strips above 60° and below −60° fill 33% of the rectangle, but hold only 13% of the hemisphere, and the strip above 80° fills 5.6% of the map for 0.76% of the directions.

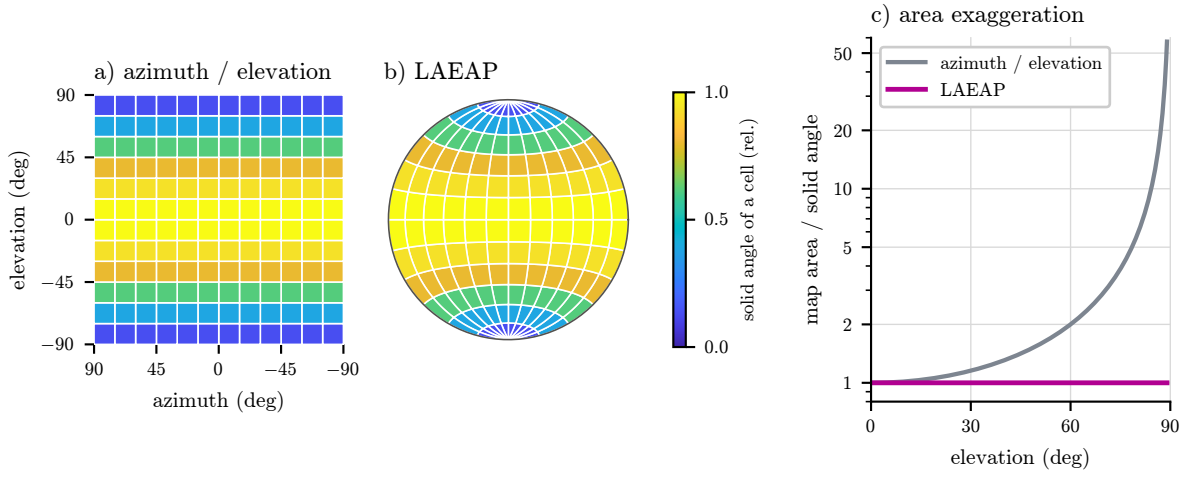


Figure 2: The same 15° azimuth/elevation cells on a) the rectangular map and b) the LAEAP disc, coloured by the solid angle they hold (relative to a cell at the horizon). On the rectangle, all cells look the same; on the disc, their area is their solid angle. c) How much too large the map draws a patch of sky, against elevation.

Key idea 1

On an azimuth/elevation map, a cell of $d\phi\, d\theta$ holds the solid angle $\cos\theta\, d\phi\, d\theta$. The map exaggerates everything at high elevation by $1/\cos\theta$, and stretches each pole, a single direction, into a whole edge of the map.

4 A Map That Keeps Area

We now build a map in which area on the map equals solid angle on the sphere. Two choices make the derivation short. First, we centre the map on boresight, the x axis, since that is where a sonar or an ear looks. Second, we use polar coordinates around boresight: t is the angle between $\boldsymbol{d}$ and the x axis, and ψ the angle around it. The map is azimuthal, which means that a direction with angles (t, ψ) goes to the point at radius $r(t)$ and angle ψ on the page. Directions at the same angle from boresight end up on the same circle, and the only freedom left is the function $r(t)$.

On the sphere, the same argument as before gives the solid angle of a small cell dt by $d\psi$. A step dt moves along a great circle and covers dt. A step $d\psi$ moves along a circle of constant t, of radius $\sin t$, and covers $\sin t\, d\psi$. So

$$d\Omega = \sin t\; dt\, d\psi. \tag{7}$$

On the page, the cell becomes a piece of a ring, dr wide and $r\, d\psi$ long, with area

$$dA = r\, dr\, d\psi = r\, \frac{dr}{dt}\, dt\, d\psi. \tag{8}$$

For an equal-area map, $dA = d\Omega$ for every cell, so the radius must satisfy

$$r\, \frac{dr}{dt} = \sin t, \qquad \text{that is} \qquad \frac{d}{dt}\left(\frac{r^2}{2}\right) = \sin t. \tag{9}$$

Boresight itself must go to the centre, $r(0) = 0$. Integrating from 0 to t then gives

$$\frac{r^2}{2} = 1 - \cos t = 2\sin^2\frac{t}{2} \qquad \Longrightarrow \qquad r = 2\sin\frac{t}{2}. \tag{10}$$

This is the Lambert azimuthal equal-area projection, introduced by Johann Heinrich Lambert in 1772. The radius has a simple geometric meaning: $2\sin(t/2)$ is the length of the straight chord from the boresight point $(1, 0, 0)$ on the unit sphere to the point $\boldsymbol{d}$ (Fig. 3a). The map rotates every such chord about the boresight point down onto the plane that touches the sphere there.

The rim of the frontal hemisphere, $t = 90°$, lands at $r = 2\sin 45° = \sqrt{2}$, so the hemisphere fills a disc of radius $\sqrt{2}$. Its area is $\pi(\sqrt{2})^2 = 2\pi$, exactly the solid angle of the hemisphere, as it must be. In Cartesian form, which is what our code uses (`common/laeap.py`), the map needs no angles at all. With $\sin t = \sqrt{d_y^2 + d_z^2}$ and $\cos t = d_x$, the point $\boldsymbol{d}$ goes to

$$(X, Y) = \sqrt{\frac{2}{1 + d_x}}\; (-d_y,\; d_z), \tag{11}$$

where the minus sign puts the sensor's left on the left, as if we looked over its shoulder. The inverse, from a pixel (X, Y) back to a direction, follows from $t = 2\arcsin(\rho/2)$ with $\rho = \sqrt{X^2 + Y^2}$, and that is how we build a pixel grid of directions for beamforming.

An equal-area map cannot keep shapes as well. Along the radius, the map scale is $dr/dt = \cos(t/2)$. Along a circle of constant t, it is the ratio of the circle on the page to the circle on the

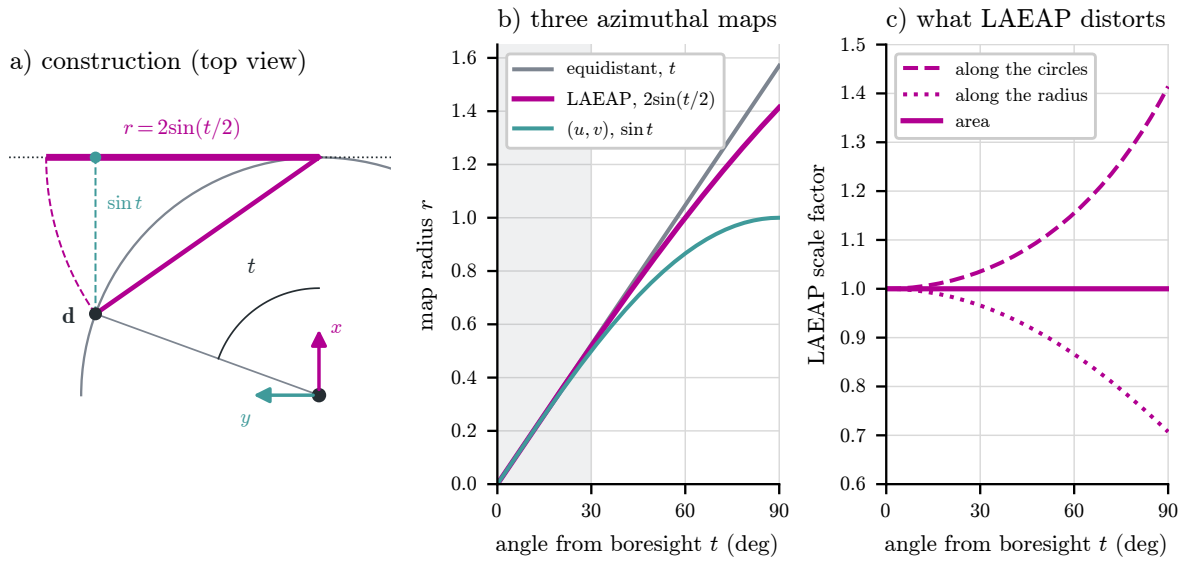


Figure 3: a) The construction of the LAEAP, in the horizontal plane through the sensor (triad: x forward, magenta, y left, teal). A direction $\boldsymbol{d}$ at angle t from boresight goes to the radius r equal to the chord from the boresight point to $\boldsymbol{d}$ (magenta). The direction-cosine map uses the perpendicular distance $\sin t$ instead (teal). b) The map radius against t for three azimuthal maps. Within $\pm 30°$ (grey band) they nearly coincide. c) The local scale of the LAEAP along the circles of constant t and along the radius. Their product, the area scale, is 1 everywhere.

sphere, $r/\sin t = 1/\cos(t/2)$. The product is 1, which is the equal-area property, but the two factors differ away from the centre (Fig. 3c). At 30° from boresight they are 0.97 and 1.04, and shapes are almost unchanged. At the rim they are 0.71 and 1.41, so a small circle of directions near the rim is drawn as an ellipse twice as long along the rim as across it. The LAEAP squeezes shapes near the rim, and that is the price it pays for keeping area everywhere.

Key idea 2

Requiring map area to equal solid angle, $r\,dr = \sin t\,dt$, fixes the map radius to $r = 2\sin(t/2)$, the chord from boresight to the direction. The frontal hemisphere becomes a disc of radius $\sqrt{2}$ and area 2π. Shapes are kept near the centre and squeezed by up to a factor 2 near the rim.

5 What Equal Area Buys

Energy at its true size

A sonar image, a beampattern in power and an HRTF are all densities over directions. When we look at such a map, we judge how much energy sits somewhere by the brightness and the area of a bright patch. On an equal-area map that judgement is correct, because the integral of the map over a region is the energy from the directions in that region. On the rectangular map it is biased towards the poles. For the broadside beam of Fig. 1, only 2.2% of the energy arrives from elevations above 60° or below −60°, but those regions hold 5.3% of the energy as the rectangular picture shows it. Strong reverberation from a ceiling or a floor would look more than twice as important as it is.

A uniform set of beams

A beamformer has to choose the directions it computes, and the cost of an image is proportional to their number. The natural choice is one direction per pixel of the map we will look at. On a rectangular grid with spacing δ in azimuth and elevation, the frontal hemisphere needs $(180°/\delta + 1)^2$ directions. Near the poles, neighbouring directions in azimuth are only $\delta \cos\theta$ apart, much closer than the beam is wide, so many of them are computed for nothing. The third of the grid above 60° and below −60° covers only 13% of the directions. On a square LAEAP pixel grid with spacing δ (in radians, the same as an angle near the centre), every pixel holds the same solid angle δ^2, and the hemisphere needs about $2\pi/\delta^2$ pixels. Rectangular map area is $\pi \times \pi$ for the hemisphere, so the rectangular grid needs $\pi^2/2\pi = \pi/2 \approx 1.57$ times as many directions for the same resolution at the horizon. At $\delta = 1°$, that is 32,761 directions against 20,641 (Fig. 4), and LAEAP saves 37% of the beamforming effort for every image. The saved directions are all near the poles, where the rectangular grid oversamples. Near the rim, a LAEAP pixel is $1.41\,\delta$ long in the direction away from boresight and $0.71\,\delta$ across, which suits a planar array, whose beam widens in that same direction.

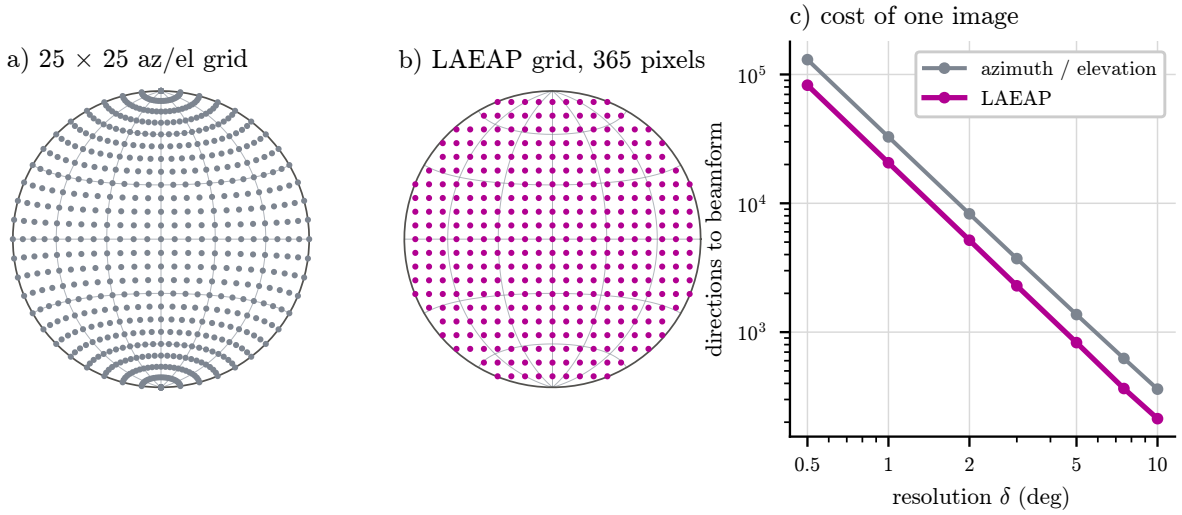


Figure 4: Choosing the directions to beamform. a) A rectangular grid with 7.5° spacing (625 directions), drawn on the LAEAP disc: the directions crowd together at the poles. b) A square LAEAP pixel grid with the same spacing at the centre (365 directions), with one pixel per equal solid angle. c) The number of directions for the frontal hemisphere against the resolution δ. The two lines are a factor of about $\pi/2$ apart.

No seams

The frontal hemisphere is one disc, and the poles of the azimuth/elevation system are ordinary points on it, so a beam or an echo can pass over them in one piece. On the rectangle, a feature that crosses a pole is cut in two.

6 Worked Example: the Steered Beam

We return to the 8×8 array of Fig. 1 and measure its −3 dB mainlobe on each map. We find the true solid angle of the mainlobe by summing equation (6) over the pixels of a fine azimuth/elevation grid. Broadside, the mainlobe covers 40 msr. All three maps draw it at that size and as a round spot, since near boresight they are all the same map.

Steered to $(55°, 45°)$, the mainlobe covers 118 msr, 3.0 times more. This growth is physical and would show up on any map. Seen from 66° off boresight, the array looks foreshortened by $\cos t = 0.41$, so its beam is about $1/\cos t$ wider in the direction away from boresight, and a little more because the beam is wide enough for $\cos t$ to vary across it. Each map shows this differently:

- The LAEAP draws the mainlobe with an area of 118 msr, 1.00 times its solid angle, as it must. Its long axis is 2.0 times its short axis, radially stretched, because the beam really is wider in that direction.
- The rectangular map draws it 1.47 times too large and 4.1 times longer than wide, bent along the circle of 45° elevation.
- The direction-cosine map keeps the shape of the broadside lobe (ratio 1.1), but draws it at only 0.31 of its solid angle. The beam has grown, and this map hides that. Part of the lobe even falls outside $u^2 + v^2 \leq 1$, where there are no real directions.

Only the LAEAP lets us read off from the picture how much of the sky the beam covers, and the clutter and reverberation a beam collects grow with exactly that solid angle.

Key idea 3

A steered beam really covers more directions than a broadside beam, about $1/\cos t$ more. The LAEAP shows it at its true size, the rectangular map exaggerates and bends it, and the direction-cosine map hides the growth.

7 Real Bat Ears

An array beam is a clean test case, but the maps we draw most often are HRTFs. Figure 5 shows the left-ear HRTF of *Phyllostomus discolor*, the same one as in note 1. It was computed with the boundary element method on a CT scan of the head and covers 25 to 95 kHz. We scale each frequency to its own maximum. The acoustic axis (white cross) points 42.5° to the left and 7.5° up at 30 kHz. At higher frequencies it moves closer to the front and stays near the horizon, at (22.5°, 2.5°) at 70 kHz and (30°, −2.5°) at 90 kHz. The main lobe narrows with frequency, as an antenna of fixed size must. Its −6 dB region covers 1.52 sr at 30 kHz, 0.60 sr at 50 kHz and only 0.20 sr at 90 kHz, 7.6 times less than at 30 kHz. On the LAEAP disc, these areas can be compared by eye.

Because the acoustic axis of this ear lies close to the horizon, the rectangular map draws the main lobe nearly at its true size, 1.10 times too large at 30 kHz and 1.07 times at 50 kHz. The distortion sits in the rest of the pattern (Fig. 5e,f). The top and bottom rows of the rectangle each show one direction, stretched over the full width, and the weak structure at high elevations is spread out sideways. Summed over the map, the region above 60° and below −60° elevation holds 4.4% of the ear's sensitivity (its power integrated over solid angle) at 30 kHz, but 12.3% of it as the rectangle shows it. At 50 kHz the numbers are 4.1% and 13.9%. A reader who compares how much the ear hears from above with how much it hears from the side gets an answer that is off by a factor of 2.8 to 3.4.

Bats also move their ears, and the LAEAP makes the effect easy to read. Figure 6 shows the left ear of *Micronycteris microtis* at 40 kHz, with both pinnae tilted forward by 20°, at rest, and tilted back by 25°, each pose computed again with the boundary element method. Tilting the pinnae moves the main lobe of the ear by up to 18° at this frequency. On the discs this is a shift of a lobe of roughly constant size, with the graticule still in place to read off where it went.

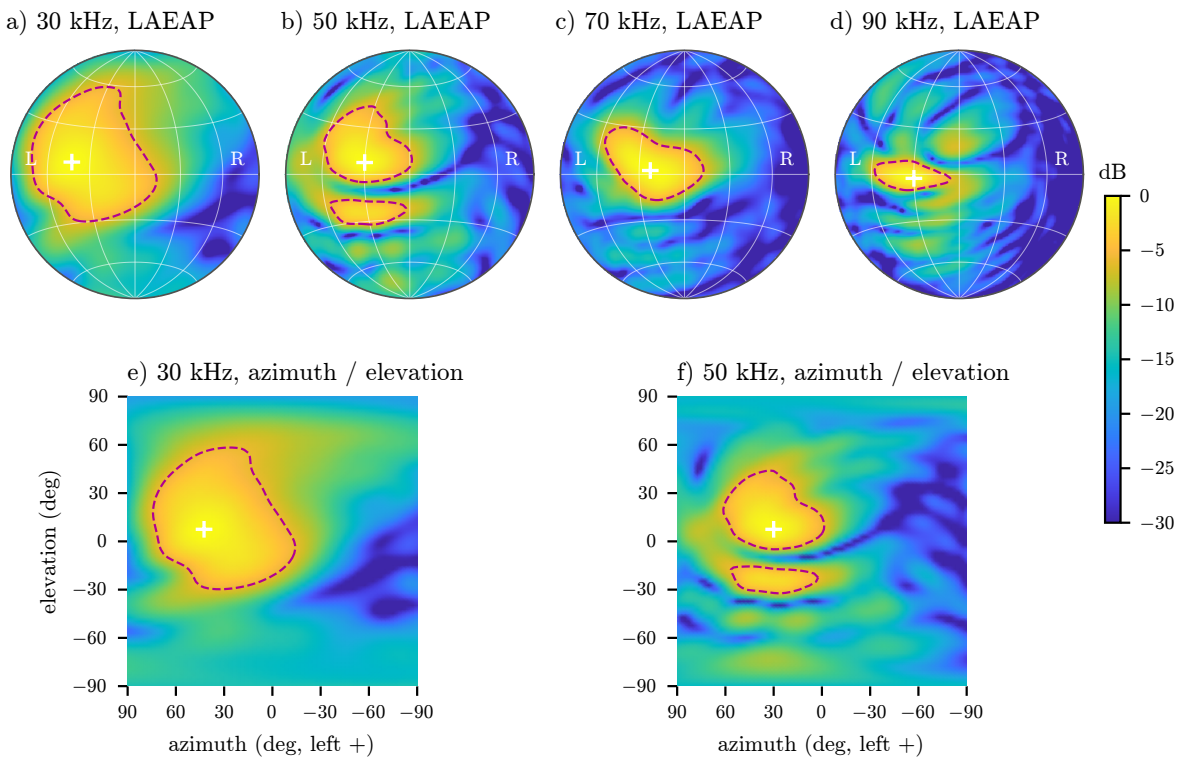


Figure 5: The left-ear HRTF of *P. discolor* (boundary element method on the CT mesh, Bat ERTF Meshes dataset), each frequency in dB relative to its own maximum. a–d) LAEAP discs at four frequencies, seen from behind the bat. e, f) The same data at 30 and 50 kHz on the azimuth/elevation map. The magenta contour is the −6 dB region, the white cross the acoustic axis.

8 When the Choice Matters

How much the map matters depends on the field of view. Within 30° of boresight, the LAEAP radius $2\sin(t/2) = 0.518$ differs from the direction-cosine radius $\sin t = 0.500$ by only 3.5%, and the rectangular map exaggerates area by at most 1.15 at its top and bottom edges. For a

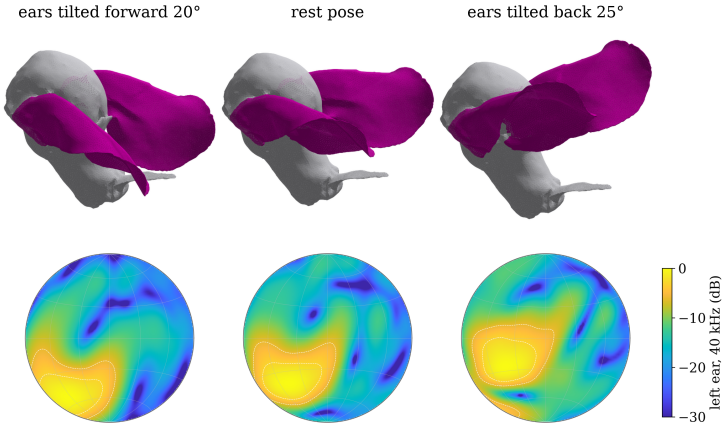


Figure 6: The head of *Micronycteris microtis* with both pinnae (magenta) tilted forward by 20°, at rest, and tilted back by 25°, and below each pose the left-ear pattern at 40 kHz as a LAEAP disc (seen from behind the bat, contours at −3 and −6 dB). From the Medium post *Seven bat heads, and what they do to sound*, computed from the Bat ERTF Meshes dataset.

narrow-field device such as an acoustic leak camera, which images about ±30°, every map gives nearly the same picture, and the choice is a matter of taste.

Our sensors are different. The eRTIS images the whole frontal hemisphere, and HiRIS, with its 1024 microphones on a 32×32 grid, makes 3D images of the same kind. A bat's ear, too, hears the whole frontal hemisphere and more. Here the rectangular map exaggerates area by 2.0 at 60° and 5.8 at 80° elevation, and the choice of map changes what the reader sees. We therefore draw all our 3D sonar images, beampatterns and HRTFs in the LAEAP, with the same conventions: the centre is straight ahead, the rim is 90° away, the hemisphere is seen from behind the sensor (or the bat), so that left is on the left, and white grid lines mark every 30° of azimuth and elevation, as in note 1.

Other azimuthal maps keep other properties. The azimuthal equidistant map, $r = t$, keeps the angle from boresight along every radius, and puts the rim at $r = \pi/2$, but it draws the rim area 1.57 times too large. The stereographic map, $r = 2\tan(t/2)$, keeps the shape of small features everywhere (it is conformal), but draws the rim area 4 times too large. The direction-cosine map, $r = \sin t$, keeps the beampattern of a planar array shift-invariant, but shrinks the rim to nothing. All four agree near boresight, and only the LAEAP keeps the one property an energy map needs, that equal areas hold equal amounts of sky.

Exercise

1. Show that an azimuth/elevation cell from θ_1 to θ_2 and $\Delta\phi$ wide holds the solid angle $\Delta\phi(\sin\theta_2 - \sin\theta_1)$. How many times more solid angle does a 5° cell at the horizon hold than the 5° cell next to the pole?
2. Derive the area scale of the azimuthal equidistant map, $r = t$, and of the stereographic map, $r = 2\tan(t/2)$, at angle t from boresight. Check the values 1.57 and 4 at the rim.
3. Applied to the whole sphere, equation (10) gives a disc of radius 2. Where does the direction straight behind the sensor end up, and why is that a problem for an image of the full sphere?
4. An eRTIS image is beamformed at 2° resolution over the frontal hemisphere. How many directions does a rectangular grid need, and how many a LAEAP grid? If one direction takes 10 μs on a GPU, how many images per second does each grid allow?

Further Reading

- J. P. Snyder, *Map Projections: A Working Manual*, U.S. Geological Survey Professional Paper 1395, 1987. History, formulas and distortion of the LAEAP.
- H. L. Van Trees, *Optimum Array Processing*, Wiley, 2002. Beampatterns of planar arrays in direction cosines (u-v space).
- W. Jansen, W. Daems and J. Steckel, "Delay-multiply-and-sum beamforming for real-time in-air acoustic imaging," arXiv:2511.09165, 2025. Point-spread functions of the eRTIS shown in the LAEAP.
- R. Kerstens, D. Laurijssen and J. Steckel, "eRTIS: A fully embedded real time 3D imaging sonar sensor for robotic applications," IEEE ICRA, 2019.
- J. Steckel, "Full-sphere emission and reception directivities of seven echolocating bat species," submitted, 2026. Data: https://doi.org/10.5281/zenodo.23729269. The source of the bat HRTFs above.